submit stencil

• ARTICLES •

A new oligobenzodithiophene end-capped with 3-ethyl-rhodanine groups for organic solar cells with high open-circuit voltage

NI Wang, LI MiaoMiao, WAN XiangJian,* ZUO Yi, KAN Bin, FENG HuanRan, ZHANG Qi-an, & CHEN YongSheng*

Key Laboratory of Functional Polymer Materials, Collaborative Innovation Center of Chemical Science and Engineering (Tianjin), Center for Nanoscale Science and Technology, Institute of Polymer Chemistry, College of Chemistry, Nankai University, Tianjin 300071, China

*Corresponding authors (yschen99@nankai.edu.cn, xjwan@nankai.edu.cn)

A new solution-processable small-molecule donor material, named DRBDT₃, comprised of oligobenzo[1,2-b:4,5-b'] dithiophene as the backbone and 3-ethyl-rhodanine as the end-capped group has been designed and synthesized for application in organic photovoltaic cells. The oligobenzodithiophene derivative exhibits an absorption band from 300 to 640 nm. The film of DRBDT₃ shows highly long-range ordering assembly and high mobility of 1.21×10^{-4} cm^2 V^{-1} s^{-1}. The new molecule shows a deep highest-occupied molecular orbital energy level. The device based on DRBDT₃ as the donor and PC$_{71}$BM as the acceptor exhibits a power conversion efficiency of 4.09% with a high open-circuit voltage of 0.99 V under AM.1.5G illumination (100 mWcm^{-2}).

Keywords: small molecule, organic solar cell, oligobenzodithiophene, high open-circuit voltage

1   Introduction

Organic photovoltaic cells (OPVs) have attracted an increasing amount of attention during the past decade, due to their advantages of solution processability, light weight, low cost, and potential in the fabrication of flexible devices [1-9]. Many efforts have been made to improve the power conversion efficiency (PCE) of polymer-based OPVs (P-OPVs) [10-15] PCEs over 9% have been achieved [16-21] in the past few years. Compared to polymer materials, small molecules exhibit competitive advantages such as well-defined structure and therefore less batch-to-batch variation, easier band structure control, etc. [22-31]. To date, solution-processed small-molecule-based OPVs (SM-OPVs) have achieved PCEs higher than 8% [32-35] through design and synthesis of new small- molecule materials and optimization of device fabrication [36-41].

Benzo[1,2-b:4,5-b'] dithiophene (BDT) as an electron-donating unit has been widely used in P-OPVs

[3,42-45]. The symmetric and plain conjugated structure could facilitate the formation of π-π stacking. Devices based on BDT-based polymer are able to afford high PCEs of more than 9% [16, 17]. A series of BDT-based polymers including homopolymers and copolymers has been reported by Yang's group [40]. Among these BDT-based polymers, BDT-based homopolymer shows the deepest highest-occupied molecular orbital (HOMO) energy level, which could lead to a high V$_{oc}$ in OPV devices because open circuit voltage (V_{oc}) mainly depends on the difference between the HOMO energy level of the donor material and the lowest unoccupied molecular orbital (LUMO) energy level of the acceptor material [5, 46]. John P. Ferraris *et al.* reported a BDT-based homopolymer, named O-PBDT, which exhibits a PCE of 1.56% with a high V$_{oc}$ of 0.83 V and a relatively low short-circuit current density (J_{sc}) of 4.18 mA cm^{-2} [47]. The relatively low J_{sc} of O-PBDT is believed to be due to the narrow absorption band with absorption onset at 560 nm. To enhance the J_{sc}, it is essential to reduce the band gap, which is decided by the difference between the HOMO en-

followed by the addition of Pd(PPh$_3$)$_4$ (30 mg, 0.026 mmol). After stirring at 100°C for 24 h under argon, the mixture was poured into water (200mL) and extracted with chloroform. The organic layer was washed with water and then dried over anhydrous Na$_2$SO$_4$. The solvent was removed under reduced pressure and the residue was purified by silica gel chromatography using a mixture of petroleum and dichloromethane ether (1:2) as eluant to afford compound DCHOBDT$_3$ (1.22 g, 68%). ^{1}H NMR (400 MHz, CDCl$_3$): δ 9.94 (s, 2H), 7.95 (s, 2H), 7.44 (s, 4H), 4.20 (m, 12H), 1.90–1.40 (m, 54H), 1.35–0.90 (m, 36H). ^{13}C NMR(100 MHz, CDCl$_3$): δ 184.24, 146.44, 144.34, 144.25, 142.35, 138.74, 136.25, 135.39, 132.62, 131.77, 131.46, 130.59, 129.41, 128.44, 118.60, 117.59, 40.71, 30.49, 30.45, 30.37, 29.73, 29.32, 29.29, 29.24, 23.89, 23.83, 23.23, 23.18, 14.33, 14.27, 14.24, 11.41, 11.39. MS (MALDI-TOF): calcd for C$_{80}$H$_{110}$O$_8$S$_6$ [M$^+$], 1390.65; found: 1390.65.

Synthesis of DRBDT$_3$

To a CHCl3 (60 mL, anhydrous) solution of DCHOBDT$_3$ (0.30 g, 0.215 mmol), 3-ethyl-rhodanine (0.50 g, 3.10 mmol) and three drops of piperidine were added. The resulting solution was refluxed at 70°C for 12 h under argon. Then the mixture was poured into water (200mL) and extracted with chloroform. The organic layer was washed with water and then dried over anhydrous Na$_2$SO$_4$. The solvent was removed under reduced pressure. The residue was purified by silica gel chromatography using a mixture of petroleum and dichloromethane ether (1:1) as eluant; next, the crude solid was recrystallized using hexane and chloroform to afford DRBDT$_3$ (0.23 g, 64%). ^{1}H NMR (400 MHz, CDCl$_3$): δ 7.71 (s, 2H), 7.49 (s, 2H), 7.29 (s, 2H), 7.23 (s, 2H), 4.25–4.05 (m, 16H), 1.90–1.40 (m, 54H), 1.26 (t, 6H), 1.20–1.10 (m, 18H), 1.10–1.00 (m, 18H). ^{13}C NMR (100 MHz, CDCl$_3$): 192.01, 166.98, 145.21, 143.96, 143.78, 138.19, 136.68, 136.15, 133.01, 132.48, 131.81, 131.14, 129.20, 128.90, 128.17, 122.48, 122.33, 118.41, 117.31, 40.72, 39.86, 30.51, 30.47, 30.42, 29.37, 29.34, 29.31, 23.87, 23.30, 23.22, 14.41, 14.35, 14.29, 12.29, 11.43. MS (MALDI-TOF): calcd for C$_{90}$H$_{122}$N$_2$O$_8$S$_{10}$ [M$^+$], 1676.72; found: 1676.68.

2.4 Measurements and instruments

The H^1 and C^{13} nuclear magnetic resonance (NMR) spectra were taken on a Bruker AV400 Spectrometer. Matrix-assisted laser desorption/ionization time-of-flight (MALDI-TOF) mass spectra were performed on a Bruker Autoflex Ⅲ instrument. The transmission-electron microscope (TEM) investigation was performed on a Philips Technical G2 F20 at 200 kV. The thermogravimetric analyses (TGA) were carried out on a NETZSCH STA 409PC instrument under purified nitrogen gas flow with a 10°C min^{-1} heating rate. UV–vis spectra were obtained with a JASCO V-570 spectrophotometer. X-ray diffraction (XRD) experiments were performed on a Bruker D8 FOCUS X-ray diffractometer with Cu–Kα radiation (λ = 1.5406 Å) at a generator voltage of 40 kV and a current of 40 mA. Atomic-force microscope (AFM) investigation was performed using Bruker MultiMode 8 in tapping mode. Cyclic voltammetry (CV) experiments were performed with a LK98B Ⅱ microcomputer-based electrochemical analyzer in dichloromethane solutions. All CV measurements were carried out at room temperature with a conventional three-electrode configuration employing a glassy carbon electrode as the working electrode, a saturated calomel electrode (SCE) as the reference electrode, and a Pt wire as the counter electrode. Dichloromethane was distilled from calcium hydride under dry argon immediately prior to use. Tetrabutylammonium phosphorus hexafluoride (Bu$_4$NPF$_6$, 0.1 M) in dichloromethane was used as the supporting electrolyte; the scan rate was 100 mV s^{-1}. Hole mobility was measured by a space-charge-limited current (SCLC) method using a diode configuration of ITO/PEDOT:PSS/ donor:PC$_{71}$BM/Al by taking dark current density in the range of 0–6 V and fitting the results to a space-charge-limited form, where SCLC is described by:

$$J = \frac{9\varepsilon_0\varepsilon_r\mu_0V^2}{8L^3}\exp(0.89\beta\sqrt{\frac{V}{L}})$$

where J is the current density; L is the film thickness of the active layer; μ_0 is the hole mobility; ε_r is the relative electric constant of the transport medium; ε_0 is the permittivity of free space (8.85 × 10^{-12} F m^{-1}); V (= V_{appl} - V_{bi}) is the internal voltage of the device; V_{appl} is the applied voltage to the device; and V_{bi} is the built-in voltage due to the relative work-function difference of the two electrodes.

The current density-voltage (J-V) characteristics of th ephotovoltaic devices were obtained by a Keithley 2400 source-measure unit. The photocurrent was measured under illumination-simulated 100 mW cm^{-2} AM1.5G irradiation using a xenon-lamp-based solar simulator (Oriel 96000, AM1.5G) in an argon-filled glove box. Simulator irradiance was characterized using a calibrated spectrometer and illumination intensity was set using a certified silicon diode. The external quantum efficiency (EQE) value of the encapsulated device was obtained with a halogen-tungsten lamp, monochromator, optical chopper, and lock-in amplifier in air. Photon flux was determined by a calibrated silicon photodiode.

2.5 Fabrication of organic solar cells

The photovoltaic devices were fabricated with a structure of glass/ITO/PEDOT:PSS/donor:acceptor/ZnO/Al. The ITO-coated glass substrates were cleaned by ultrasonic treatment in detergent followed by deionized water, acetone, and isopropyl alcohol, under ultrasonication for 15 min each, and then dried by a nitrogen flow. A thin layer of PEDOT:PSS (Baytron P VP AI 4083, filtered at 0.45 μm)

was spin-coated (3000 rpm, ca. 40 nm thick) onto the ITO surface. After being baked at 150°C for 20 min, the substrates were transferred into an argon-filled glove box. Then the active layer was spin-coated from different ratios of donor (8 mg/mL):PC$_{71}$BM-blend chloroform solution at 1700 rpm for 20 s each. Next, ZnO particle suspension [49] was used to spin-coat the ZnO layer on top of the active layers. Thermal annealing was carried out on a digitally controlled hot plate at various temperatures after ZnO spin-coating in an argon-filled glove box. Finally, a 50 nm Al layer was deposited onto the ZnO film under high vacuum (< 2×10^{-4} Pa). The thickness of the ZnO and the active layer were measured using a Dektak 150 profilometer. The effective area of each cell was 4 mm^2, defined by masks for the solar-cell devices discussed in this work.

3 Results and discussion
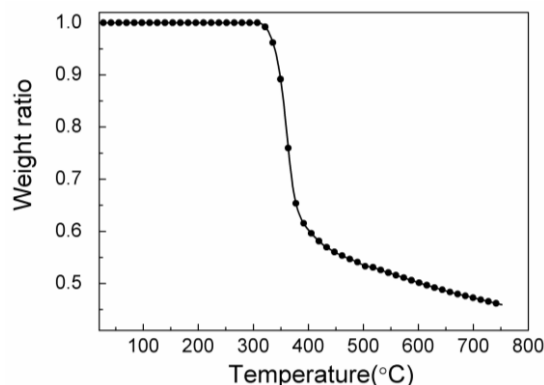
3.1 Synthesis and thermal property

Figure 1 TGA curves of DRBDT$_3$ with a heating rate of 10°C/min under N$_2$ atmosphere.

As shown in Scheme 1, the intermediate DCHOBDT$_3$ was synthesized by a Stille coupling reaction between **2** and **3** under argon atmosphere in the presence of Pd(PPh$_3$)$_4$ as the catalyst for 24 h. The target molecule DRBDT$_3$ was then prepared by the Knoevenagel condensation of DCHOBDT$_3$ with 3-ethyl-rhodanine under argon atmosphere in the presence of piperidine as the catalyst for 12 h. DRBDT$_3$ shows good solubility in common solvents. The thermal property of DRBDT$_3$ was investigated by TGA. As shown in Figure 1, compound DRBDT$_3$ exhibited good thermal stability with 5% weight-loss temperature at 337°C under N$_2$ atmosphere.

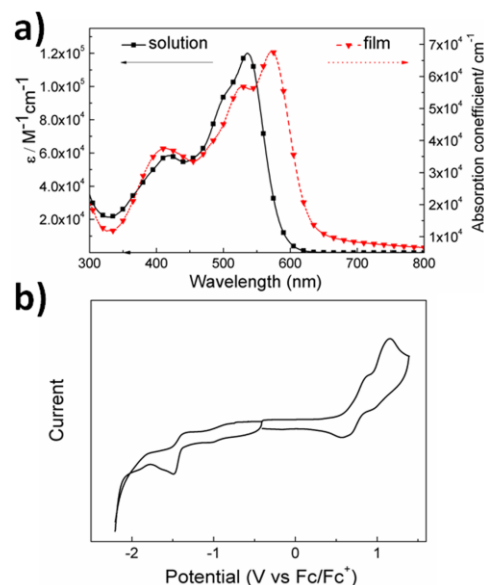## 3.2 Optical properties and electrochemical properties

Figure 2 a) Absorption spectra of DRBDT$_3$ in chloroform solution and in as-cast film; b) Cyclic voltammogram of DRBDT$_3$ in a dichloromethane solution of 0.1 mol L^{-1} TBAPF$_6$ with a scan rate of 100 mV s^{-1}.

UV–vis absorption spectra of DRBDT$_3$ in diluted chloroform solution and at solid state are shown in Figure 2a. DRBDT$_3$ in CHCl$_3$ solution shows a maximum absorption peak at 536 nm with a maximal coefficient of 1.20×10^5 M^{-1}cm^{-1}. The DRBDT$_3$ film cast from CHCl$_3$ shows a red-shifted maximum absorption peak at 572 nm with a broader absorption band from 300 to 640 nm. The optical band gap of DRBDT$_3$ is 1.97 eV, estimated from the onset of the absorption spectra. A cyclic voltammogram was used to investigate the electrochemical properties of DRBDT$_3$. Ferrocene/ferrocenium of the (Fc/Fc$^+$) redox couple (4.8 eV below the vacuum level) was used as the internal calibration. The HOMO and LUMO energy levels of DRBDT$_3$ were estimated based on the onset oxidation potential and the onset reduction potential of the redox curve as shown in Figure 2b; they are -5.34 and -3.40 eV, respectively. Note that, compared with O-PBDT, the new oligobenzodithiphene derivative end-capped with 3-ethyl-rhodanine indeed shows a decreasing LUMO energy level, which also demonstrates that the LUMO energy level of the A-D-A-structure small molecule mainly depends on the acceptor moiety. The electrochemical band gap of DRBDT$_3$ is 1.94 eV, which is consistent with the value of the optical band gap. The data for the optical and electrochemical properties are summarized in Table 1.

Table 1 Optical and electrochemical data of DRBDT$_3$.

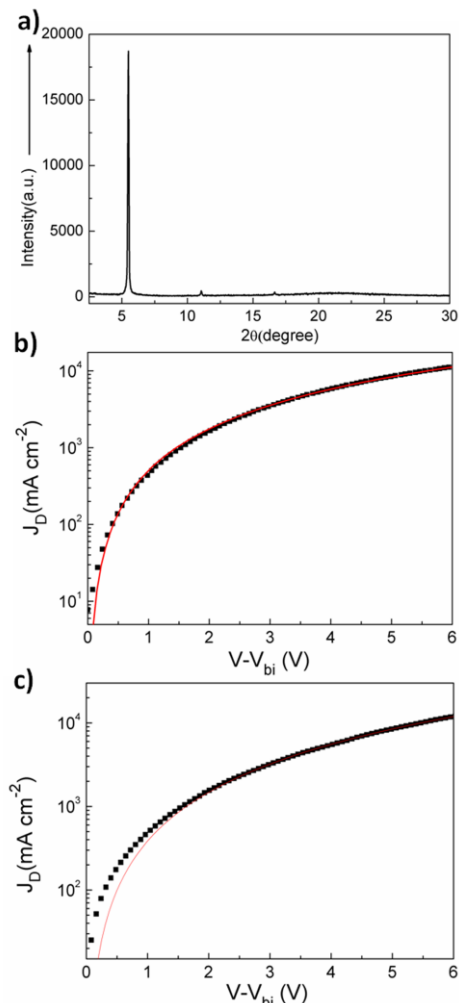| Compound	λ_{max} solution/nm	ε solution/M^{-1}cm^{-1}	λ_{max} film/nm	ε film/cm^{-1}	E_g^{opt} film/eV	E_g^{CV}/eV	HOMO/eV	LUMO/eV
DRBDT$_3$	536	1.20×10^5	572	6.8×10^4	1.97	1.94	-5.34	-3.40

3.3 X-Ray diffraction (XRD) and mobility

Figure 3 a) XRD pattern of pristine DRBDT₃ film spin-coated from CHCl₃ onto the glass substrate. b) *J-V* characteristics of a hole-only device with the configuration ITO/PEDOT:PSS (30 nm)/DRBDT₃:PC₇₁BM/Au (30 nm). c) *J-V* characteristics of a electron-only device with the configuration ITO/Al (30 nm)/DRBDT₃:PC₇₁BM /Al (30 nm). The solid line represents the fit using a model of single-carrier SCLC with field-independent mobility. The J_D-V characteristics are corrected for the built-in voltage V_{bi} that arises from the work-function difference between the contacts.

The structural order of the pristine DRBDT₃ film spin-coated from CHCl₃ solution was investigated by XRD analysis. As shown in Figure 3a, we observed a strong diffraction peak at 2θ=5.49°, corresponding to a d_{100}-spacing value of 16.09 Å for first order. The d_{100}-spacing value is the distance between the planes of the main conjugation chains of DRBDT₃, which are separated by alkyloxy side-chains. The second- and third-order diffraction peaks, at 2θ=11.05° and 16.65°, are also clearly evident. The results of XRD show that DRBDT₃ has some long-range ordering at the solid state. The hole mobility of DRBDT₃/PC₇₁BM (w/w, 1:0.8) blend film was measured by SCLC method. As plotted in Figures 3b and 3c,

the calculated hole mobility and electron mobility of the blend films were 1.21×10^{-4} cm²V⁻¹S⁻¹ and 1.43×10^{-4} cm²V⁻¹S⁻¹, respectively. The blend films showed balanced hole and electron transport which could be beneficial for charge collection. The high hole mobility of DRBDT₃ was ascribed to the strong and ordered packing of DRBDT₃, as demonstrated by the XRD results above.
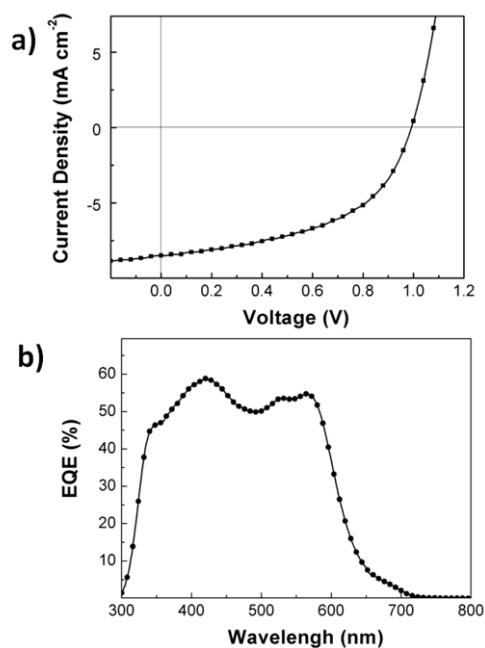
3.4 Photovoltaic properties

Figure 4 a) *J-V* curve of optimized device based on DRBDT₃:PC₇₁BM (1:0.8, w/w); b) EQE of devices based on DRBDT₃:PC₇₁BM (1:0.8, w/w) with or without thermal annealing.

Table 2 Device-performance parameters of the BHJ solar cells based on DRBDT₃:PC₇₁BM-blend films with different donor:accpetor blend ratios.

Blend ratio	V_{oc}/V	J_{sc}/mA cm⁻²	FF	PCE (%)
1:0.5	0.98	7.90	0.48	3.72
1:0.8	0.99	8.26	0.50	4.09
1:1	0.99	7.96	0.49	3.86

SM-OPV devices were fabricated using DRBDT₃ as the electron donor material and PC₇₁BM as the electron acceptor material with a conventional device structure of glass/ITO/PEDOT:PSS/DRBDT₃:PC₇₁BM/ZnO/Al, using the solution spin-coating process. The typical *J-V* curve of the test results is displayed in Figure 4a and the results are summarized in Table 2. The optimized device based on DRBDT₃:PC₇₁BM-blend film shows a PCE of 4.09% with a high V_{oc} of 0.99 V, a J_{sc} of 8.26 mA cm⁻² and *FF* of 0.50. The high V_{oc} of the device based on DRBDT₃ is consistent with its deep HOMO energy level. The external quantum efficiency (EQE) spectrum of the optimized device is shown in Figure 4b. From the EQE curve, we can see that the DRBDT₃-based device exhibits a moderate response, from 330 nm to 640 nm, with the maximum EQE value of 58% at 420 nm.
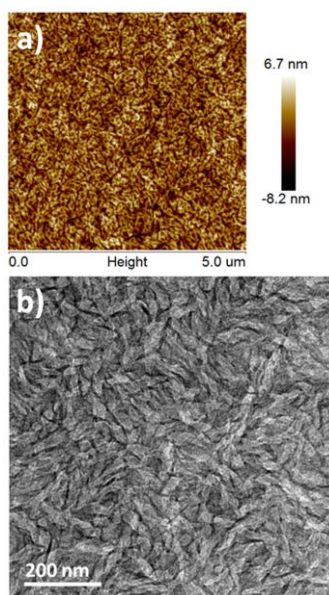
3.5 Morphology of the DRBDT₃:PC₇₁BM-blend film

Figure 5 AFM (a) and TEM (b) images of DRBDT₃:PC₇₁BM-blend film.

The morphology of DRBDT₃:PC₇₁BM blend film was investigated by atomic-force microscopy (AFM) and transmission-electron microscopy (TEM). As shown in Figure 5a, root mean square (*rms*) roughness of DRBDT₃:PC₇₁BM blend film was 1.72 nm. The surface of the blend film was uniform and smooth, indicating the good film quality of the DRBDT₃:PC₇₁BM-blend film. From Figure 5b, we can see that the DRBDT₃:PC₇₁BM film exhibited an interpenetrating network with the width of 50~60 nm. The domain size is much larger than the ideal charge diffusion length (10~20 nm), [50] leading to relatively low photocurrent, which is consistent with the result of EQE.

4   Conclusions

In conclusion, we designed and synthesized a new oligo-benzo[1,2-b:4,5-b'] dithiophene derivative comprising of three benzo[1,2-b:4,5-b'] dithiophene units as the central building block and 3-ethyl-rhodanine as terminal units. The new molecule shows a broad absorption, from 300 to 640 nm, and a deep HOMO energy level of -5.34 eV. The optimal device based on DRBDT₃/PC₇₁BM-blend film shows a PCE of 4.09% with a high V_{oc} of 0.99V, a short-circuit current of 8.26 mA cm⁻², and a fill factor of 0.50. Furthermore, this new oligobenzo[1,2-b:4,5-b'] dithiophene derivative exhibits a much better photovoltaic performance than BDT-based homopolymer. These results demonstrate that oligo-benzodithiophene derivatives would be potential small-molecule donor materials for OPVs.
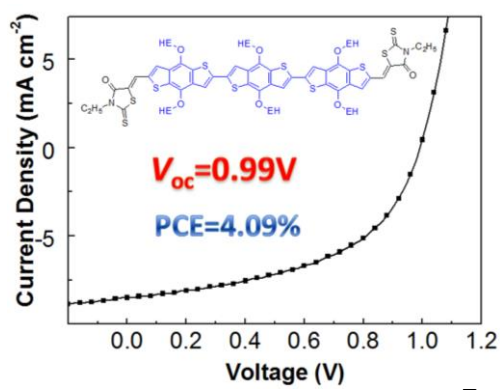
[1]   Chen JW, Cao Y. Development of novel conjugated donor polymers for high-efficiency bulk-heterojunction photovoltaic devices. *Acc Chem Re.*, 2009, 42: 1709-1718

[2]   Li YF. Molecular design of photovoltaic materials for polymer solar cells: Toward suitable electronic energy levels and broad absorption. *Acc Chem Res*, 2012, 45: 723-733

[3]   Ye L, Zhang SQ, Huo LJ, Zhang MJ, Hou JH. Molecular design toward highly efficient photovoltaic polymers based on two-dimensional conjugated benzodithiophene. *Acc Chem Res*, 2014, 47: 1595-1603

[4]   Heeger AJ. Semiconducting polymers: The third generation. *Chem Soc Rev*, 2010, 39: 2354-2371

[5]   Scharber MC, Mühlbacher D, Koppe M, Denk P, Waldauf C, Heeger, AJ, Brabec, CJ. Design rules for donors in bulk-heterojunction solar cells-towards 10 % energy-conversion efficiency. *Adv Mater*, 2006, 18: 789-794

[6]   Duan CH, Wang CD, Liu SJ, Huang F, Choy CHW, Cao Y. Two-dimensional like conjugated copolymers for high efficiency bulk-heterojunction solar cell application: Band gap and energy level engineering. *Sci China Chem*, 2011, 54: 685-694

[7]   Arias AC, MacKenzie JD, McCulloch I, Rivnay J, Salleo A. Materials and applications for large area electronics: Solution-based approaches. *Chem Rev*, 2010, 110: 3-24

[8]   Chen H-Y, Hou JH, Zhang SQ, Liang YY, Yang GW, Yang Y, Yu LP, Wu Y, Li G. Polymer solar cells with enhanced open-circuit voltage and efficiency. *Nat Photon*, 2009, 3: 649-653

[9]   Qian D, Ma W, Li ZJ, Guo XG, Zhang SQ, Ye L, Ade H, Tan ZA, Hou JH. Molecular design toward efficient polymer solar cells with high polymer content. *J Am Chem Soc*, 2013, 135: 8464-8467

[10]   Deng YF, Bao BX, Tian HK, Xie ZY, Geng YH. Synthesis of conjugated polymers based on dithieno[3,2-*b*:2',3'-*d*] phosphole oxides and their applications in thin-film transistors and bulk heterojunction solar cells. *Acta Polym Sinica*, 2013, 0: 609-618

[11]   Deng YF, Liu JW, Wang JT, Liu LH, Li WL, Tian HK, Zhang XJ, Xie ZY, Geng YH, Wang FS. Dithienocarbazole and isoindigo based amorphous low bandgap conjugated polymers for efficient polymer solar cells. *Adv Mater*, 2014, 26: 471-476

[12]   Xiao ZG, Yuan YB, Yang B, VanDerslice J, Chen JH, Dyck O, Duscher G, Huang JS. Universal formation of compositionally graded bulk heterojunction for efficiency enhancement in organic photovoltaics. *Adv Mater*, 2014, 26: 3068-3075

[13]   Yang TB, Qin DH, Lan LF, Huang WB, Gong X, Peng JB, Cao Y. Inverted polymer solar cells with a solution-processed zinc oxide thin film as an electron collection layer. *Sci China Chem*, 2012, 55: 755-759

[14]   Yang SP, Zhang Y, Jiang T, Sun XF, Lu CQ, Li G, Li XW, Fu GS. Enhancing the power conversion efficiency of pcdtbt:Pc₇₁bm polymer solar cells using a mixture of solvents. *Chin Sci Bull*, 2014, 59: 297-300

[15]   Song HY, Tong H, Xie ZY, Wang LX, Wang FS. Synthesis, characterization and solar cell application of a D-A copolymer with cyclopentadithiophene and fluorene as donor units. *Chin J Polym Sci*, 2013, 31: 1117-1126

[16]   He ZC, Zhong CM, Su SJ, Xu M, Wu HB, Cao Y. Enhanced power-conversion efficiency in polymer solar cells using an inverted device structure. *Nat Photon*, 2012, 6: 591-595

[17]   Guo X, Zhang MJ, Ma W, Ye L, Zhang SQ, Liu SJ, Ade H, Huang F, Hou JH. Enhanced photovoltaic performance by modulating surface composition in bulk heterojunction polymer solar cells PBDTTT-C-T/PC₇₁BM. *Adv Mater*, 2014, 26: 4043-4049

[18]   Zhang WJ, Wu YL, Bao QY, Gao F, Fang JF. Morphological control for highly efficient inverted polymer solar cells via the backbone design of cathode interlayer materials. *Adv Energy Mater*, 2014, DOI: 10.1002/aenm.201400359

[19]   Liao S-H, Jhuo H-J, Cheng Y-S, Chen S-A. Fullerene derivative-doped zinc oxide nanofilm as the cathode of inverted polymer solar cells with low-bandgap polymer (PTB7-TH) for high performance. *Adv Mater*, 2013, 25(34): 4766-4771

[20]   You JB, Dou LT, Yoshimura K, Kato T, Ohya K, Moriarty T, Emery K, Chen C-C, Gao J, Li G, Yang Y. A polymer tandem solar cell with 10.6% power conversion efficiency. *Nat Commun*, 2013, 4,1446

[21]   Ye L, Zhang SQ, Zhao WC, Yao HF, Hou JH. Highly efficient 2d-conjugated benzodithiophene-based photovoltaic polymer with linear

alkylthio side chain. *Chem Mater*, 2014, 26: 3603-3605

[22] Lin YZ, Zhang Z-G, Bai HT, Li YF, Zhan XW. A star-shaped oligothiophene end-capped with alkyl cyanoacetate groups for solution-processed organic solar cells. *Chem Commun*, 2012, 48: 9655-9657

[23] Zeng SH, Yin LX, Ji CY, Jiang XY, Li KC, Li YQ, Wang Y. D-π-A-π-D type benzothiadiazole-triphenylamine based small molecules containing cyano on the π-bridge for solution-processed organic solar cells with high open-circuit voltage. *Chem Commun*, 2012, 48: 10627-10629

[24] Shen SL, Jiang P, He C, Zhang J, Shen P, Zhang Y, Yi YP, Zhang ZJ, Li ZB, Li YF. Solution-processable organic molecule photovoltaic materials with bithienyl-benzodithiophene central unit and indenedione end groups. *Chem Mater*, 2013, 25: 2274-2281

[25] Lin YZ, Ma LC, Li YF, Liu YQ, Zhu DB, Zhan XW. A solution-processable small molecule based on benzodithiophene and diketopyrrolopyrrole for high-performance organic solar cells. *Adv Energy Mater*, 2013, 3: 1166-1170

[26] Gao L, Zhang J, He C, Shen SL, Zhang Y, Liu HT, Sun QJ, Li YF. Synthesis and photovoltaic properties of a star-shaped molecule based on a triphenylamine core and branched terthiophene end groups. *Sci China Chem*, 2013, 56: 997-1003

[27] Tang WL, Huang DZ, He C, Yi YP, Zhang J, Di CA, Zhang ZJ, Li YF. Solution-processed small molecules based on indacenodithiophene for high performance thin-film transistors and organic solar cells. *Org Electron*, 2014, 15: 1155-1165

[28] Chen YH, Du ZK, Chen WC, Liu Q, Sun L, Sun ML, Yang RQ. Benzo[1,2-b:4,5-b']dithiophene and benzotriazole based small molecule for solution-processed organic solar cells. *Org Electron*, 2014, 15: 405-413

[29] Yong WN, Zhang MJ, Xin XD, Li ZJ, Wu Y, Guo X, Yang Z, Hou JH. Solution-processed indacenodithiophene-based small molecule for bulk heterojunction solar cells. *J Mater Chem A*, 2013, 1: 14214-14220

[30] Qin HM, Li LS, Guo FQ, Su SJ, Peng JB, Cao Y, Peng XB. Solution-processed bulk heterojunction solar cells based on a porphyrin small molecule with 7% power conversion efficiency. *Energy Environ Sci*, 2014, 7: 1397-1401

[31] Shang HX, Fan HJ, Liu Y, Hu WP, Li YF, Zhan XW. A solution-processable star-shaped molecule for high-performance organic solar cells. Adv Mater, 2011, 23: 1554-1557

[32] Zhou JY, Wan XJ, Liu YS, Zuo Y, He GR, Long GK, Ni W, Li CX, Chen YS. Small molecules based on benzo[1,2-b:4,5-b']dithiophene unit for high-performance solution- processed organic solar cells. *J Am Chem Soc*, 2012, 134: 16345-16351

[33] Zhou JY, Zuo Y, Wan XJ, Long GK, Zhang Q, Ni W, Liu YS, Li Z, He GR, Li CX, Kan B, Li MM, Chen YS. Solution processed and high-performance organic solar cells using small molecules with a benzodithiophene unit. *J Am Chem Soc*, 2013, 135: 8484-8487

[34] Kyaw AKK, Wang DH, Wynands D, Zhang J, Nguyen, Bazan G C, Heeger A J. Improved light harvesting and improved efficiency by insertion of an optical spacer (ZnO) in solution processed small-molecule solar cells. *Nano Lett*, 2013, 13: 3796-3801

[35] Liu YS, Chen C-C, Hong ZR, Gao J, Yang YMP, Dou LT, Li G. Solution-processed small-molecule solar cells: Breaking the 10% power conversion efficiency. *Sci Rep*, 2013, 3: 3356

[36] Chen YS, Wan XJ, Long GK. High performance photovoltaic applications using solution-processed small molecules. *Acc Chem Res*, 2013, 46: 2645-2655

[37] Lin YZ, Li YF, Zhan XW. Small molecule semiconductors for high-efficiency organic photovoltaics. *Chem Soc Rev*, 2012, 41: 4245-4272

[38] Coughlin JE, Henson ZB, Welch GC, Bazan, GC. Design and synthesis of molecular donors for solution-processed high-efficiency organic solar cells. *Acc Chem Res*, 2013, 47: 257-270

[39] Lin YZ, Ma LC, Li YF, Zhu DB, Zhan XW. Small-molecule solar cells with fill factors up to 0.75 via a layer-by-layer solution process. Adv Energy Mater, 2014, 4: 1300626

[40] Liu X, Cai P, Chen DC, Chen JW, Su SJ, Cao Y. Small molecular non-fullerene electron acceptors for P3HT-based bulk-heterojunction solar cells. *Sci China Chem*, 2014, 57: 973-981

[41] Huang QL, Li HX. Recent progress of bulk heterojunction solar cells based on small-molecular donors. *Chin Sci Bull*, 2013, 58: 2677-2685

[42] Hou JH, Park M-H, Zhang SQ, Yao Y, Chen L-M, Li J-H, Yang Y. Bandgap and molecular energy level control of conjugated polymer photovoltaic materials based on benzo[1,2-b:4,5-b']dithiophene.

Macromolecules, 2008, 41: 6012-6018

[43] Liang YY, Feng DQ, Wu Y, Tsai S-T, Li G, Ray C, Yu LP. Highly efficient solar cell polymers developed via fine-tuning of structural and electronic properties. *J Am Chem Soc*, 2009, 131: 7792-7799

[44] Pan H, Wu Y, Li Y, Liu P, Ong BS, Zhu S, Xu G. Benzodithiophene copolymer-a low-temperature, solution-processed high-performance semiconductor for thin-film transistors. *Adv Funct Mater*, 2007, 17: 3574-3579

[45] Huo LJ, Hou JH, Zhang SQ, Chen H-Y, Yang Y. A polybenzo[1,2-b:4,5-b']dithiophene derivative with deep homo level and its application in high-performance polymer solar cells. *Angew Chem Int Ed*, 2010, 49: 1500-1503

[46] Zhou HX, Yang LQ, You W. Rational design of high performance conjugated polymers for organic solar cells. *Macromolecules*, 2012, 45: 607-632

[47] Lee D, Hubijar E, Kalaw GJD, Ferraris, JP. Enhanced and tunable open-circuit voltage using dialkylthio benzo[1,2-b:4,5-b']dithiophene in polymer solar cells. *Chem Mater*, 2012, 24: 2534-2540

[48] (a) He GR, Li Z, Wan XJ, Liu YS, Zhou JY, Long GK, Zhang MT, Chen YS. Impact of dye end groups on acceptor-donor-acceptor type molecules for solution-processed photovoltaic cells. *J Mater Chem*, 2012, 22: 9173-9180; (b) Long GK, Wan XJ, Kan B, Liu YS, He GR, Li Z, Zhang YW, Zhang Y, Zhang Q, Zhang MT, Chen YS. Investigation of quinquethiophene derivatives with different end groups for high open circuit voltage solar cells. *Adv Energy Mater*, 2013, 3: 639-646; (c) Li Z, He GR, Wan XJ, Liu YS, Zhou JY, Long GK, Zuo Y, Zhang MT, Chen YS. Solution processable rhodanine-based small molecule organic photovoltaic cells with a power conversion efficiency of 6.1%. *Adv Energy Mater*, 2012, 2: 74-77; (d) Schulze K, Uhrich C, Schüppel R, Leo K, Pfeiffer M, Brier E, Reinold E, Bäuerle P. Efficient vacuum-deposited organic solar cells based on a new low-bandgap oligothiophene and fullerene c60. *Adv Mater*, 2006, 18: 2872-2875

[49] Slooff WJE, Wienk MM, Kemerink M, Yang XN, Janssen RAJ. Hybrid zinc oxide conjugated polymer bulk heterojunction solar cells. *J Phys Chem C*, 2005, 109: 9505-9516

[50] (a) Yang XN, Loos J, Veenstra SC, Verhees, WJH, Wienk MM, Kroon JM, Michel MAJ, Janssen RAJ. Nanoscale morphology of high-performance polymer solar cells. *Nano Letters*, 2005, 5: 579-583; (b) Garcia-Belmonte G, Munar A, Barea EM, Bisquert J, Ugarte I, Pacios R. Charge carrier mobility and lifetime of organic bulk heterojunctions analyzed by impedance spectroscopy. *Org Electron*, 2008, 9: 847-851; (c) Peumans P, Yakimov A, Forrest SR. Small molecular weight organic thin-film photodetectors and solar cells. *Appl Phys Lett*, 2003, 93: 3693-3723

Table of Contents graphic